Ecological Indicators 121 (2021) 107062

Contents lists available at ScienceDirect

Ecological Indicators

journal homepage: www.elsevier.com/locate/ecolind

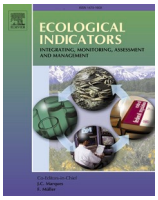

The retrieval of plant functional traits from canopy spectra through RTM-inversions and statistical models are both critically affected by plant phenology

Felix Schiefer [a,*], Sebastian Schmidtlein [a], Teja Kattenborn [a,b]

[a] Institute of Geography and Geoecology, Karlsruhe Institute of Technology (KIT), Kaiserstr. 12, 76131 Karlsruhe, Germany
[b] Remote Sensing Centre for Earth System Research, Leipzig University, Talstr. 35, 04103 Leipzig, Germany

ARTICLE INFO

Keywords:
Vegetation remote sensing
Leaf traits
PROSAIL
Partial least squares regression
Flowering
Radiative transfer model

ABSTRACT

Plant functional traits play a key role in the assessment of ecosystem processes and properties. Optical remote sensing is ascribed a high potential in capturing those traits and their spatiotemporal patterns. In vegetation remote sensing, reflectance-based retrieval methods are either statistical (relying on empirical observations) or physically-based (based on inversions of a radiative transfer model, RTM). Both trait retrieval approaches remain poorly investigated regarding phenology. However, within the phenology of a plant, its leaf constituents, canopy structure, and the presence of phenology-related organs (i.e., flowers or inflorescence) vary considerably – and so does its reflectance. We, therefore, addressed the question of how plant phenology affects the predictive performance of both statistical and RTM-based methods and how this effect differs between traits. For a complete growing season, we weekly measured traits of 45 herbaceous plant species together with hyperspectral canopy reflectance (ASD FieldSpec III). Plants were grown in an experimental setup. The investigated traits comprised Leaf Area Index (*LAI*) and the leaf traits chlorophyll, anthocyanins, carotenoids, equivalent water thickness, and leaf mass per area. We compared the predictive performances of PLSR models and three variants of PROSAIL inversions based on (1) all observations and based on (2) a phenological subset where flowering plants were excluded and only those observations most suitable for modeling were kept. Our results show that both statistical and RTM-based trait retrievals were largely affected by phenology. For carotenoids for example, R^2 decreased from 0.58 at non-flowering canopies to 0.25 at 100% flowering canopies. Temporal trends were diverse. *LAI* and equivalent water thickness were best estimated earlier in the growing season; chlorophyll and carotenoids towards senescence. PLSR models showed generally higher bias than the PROSAIL-based retrieval approaches. Lookup-table inversion of PROSAIL in combination with a continuous wavelet transformation of reflectance showed highest accuracies. We found RTM-based retrieval not to be as accurate and transferable as previously indicated. Our results suggest that phenology is essential for accurate retrieval of plant functional traits and varies depending on the studied species and functional traits, respectively.

1. Introduction

Plant functional traits are key variables for determining how plants respond to their environment (Butler et al., 2017; Díaz et al., 2016; Ustin and Gamon, 2010; von Humboldt, 1808). Capturing plant functional traits advances our understanding of ecosystem processes and properties (Jetz et al., 2016; Kunstler et al., 2016; Moreno-Martínez et al., 2018). As many functions and processes in plant canopies are directly linked to light absorption and scattering, optical remote sensing has evolved as a valuable tool to retrieve a range of plant traits in time and space. This includes leaf constituents, such as pigments, dry matter or water, or canopy properties, such as total leaf area per canopy area (Homolová et al., 2013; Kattenborn and Schmidtlein, 2019; Ustin and Gamon, 2010; Zarco-Tejada et al., 2018). Retrieval methods for functional plant traits from canopy reflectance can be grouped into statistical and physically-based approaches (Baret and Buis, 2008; Homolová et al., 2013).

Statistical methods establish empirical relationships between observed trait expressions and spectral reflectance as either parametric (e.g., vegetation indices, spectral shape) or non-parametric regressions (e.g., partial least squares regression, decision trees, support vector

* Corresponding author.
E-mail address: felix.schiefer@kit.edu (F. Schiefer).

https://doi.org/10.1016/j.ecolind.2020.107062
Received 23 June 2020; Received in revised form 18 September 2020; Accepted 8 October 2020
Available online 23 October 2020

machines). Numerous studies have reported accurate results of statistical approaches in retrieving plant traits (e.g., Asner et al., 2015; Wang et al., 2019). Statistical methods are often used exactly because they do not compulsorily require in-depth knowledge of the underlying processes and allow to model any trait as long as sufficient reference data is available and some meaningful relation to reflectance exists. Despite high accuracies and ease of implementation, statistical models are usually site-, species-, sensor-, and time-specific and thus lack transferability (but see Serbin et al., 2019). They also require – sometimes labor-intensive – sampling of calibration data and have been challenged because they replace causality by correlation, a risk inherent to empirical research that has been criticized at least since Kant (1783).

Physically-based approaches for retrieving plant traits from canopy reflectance are based on radiative transfer models (RTM). RTMs reconstruct how plant traits (e.g., pigment or water content) affect reflectance and RTM-based trait retrieval requires an inversion of this approach. RTM-inversions thus allow retrieving those traits that are incorporated in the RTM itself. Two common inversion strategies are the look-up-table approach, where traits are estimated from the correspondence of resulting RTM simulations and measured canopy reflectance, or hybrid approaches, where a statistical algorithm is trained on RTM-based simulations (Verrelst et al., 2019). RTM-based approaches are ascribed higher transferability than pure statistical approaches since their design reflects physical interactions between plant traits and electromagnetic radiation. Moreover, RTM approaches do not require reference observations for model training (Verrelst et al., 2019).

RTM-based retrieval of plant functional traits have been demonstrated in several studies (Ali et al., 2016; Atzberger et al., 2013; Darvishzadeh et al., 2008; Feilhauer et al., 2017; Kattenborn et al., 2017a; Vohland et al., 2010; Vohland and Jarmer, 2008). For a more comprehensive overview of commonly applied statistical and physically-based plant trait retrieval methods, the reader is referred to the reviews by Verrelst et al. (2019), Verrelst et al. (2015), Homolová et al. (2013) and, for grassland, by van Cleemput et al. (2018).

Despite the potential of both statistical and RTM-based remote sensing approaches for vegetation monitoring, the investigation of plant trait retrievals over time remains scarce (van Cleemput et al., 2018). However, within the phenology of a plant, its leaf constituents, canopy structure, and the presence of related organs, i.e., flowers or inflorescence, vary – and so does its reflectance (Feilhauer et al., 2016; Homolová et al., 2013; Landmann et al., 2019). It is known that the accuracy of statistical models for vegetation remote sensing can decrease when transferred to a dataset of a different phenological phase (Baret and Buis, 2008; Feilhauer and Schmidtlein, 2011). RTM-based methods should, in theory, be more time-invariant since the incorporated plant trait-reflectance relationships rely on physical principles and the latter do not change with time. However, phenological features could hamper RTMs because features such as flowers or inflorescence are not considered in the model definition. So far, both statistical and RTM-based approaches remain poorly investigated with regard to phenological variations of the studied plant traits (Danner et al., 2017; Duveiller et al., 2011; Locherer et al., 2015; Miraglio et al., 2020; Wang et al., 2019).

We hypothesize that plant phenology plays a crucial role in accurately predicting plant traits from canopy spectra. We compared trait retrieval with two common statistical and physically-based algorithms, i.e., Partial Least Squares Regression (PLSR) and the PROSAIL RTM. To analyze how plant phenology affects predictions we conducted a controlled study based on outdoor cultivated, potted graminoids and forbs. This enabled us to study multiple plant traits for an entire growing season with high temporal resolution (weekly). We compared the retrieval for those traits that are incorporated in PROSAIL and can be measured with reasonable effort, i.e., pigments (chlorophyll, carotenoid, and anthocyanin content), dry matter and water content, as well as Leaf Area Index. To assess the influence of plant phenology on model results we compared predictive performances of models based on all observations and based on a phenological subset where flowering plants were removed and only a temporal window resulting most suitable for modeling was kept. We addressed the questions of how plant phenology affects the predictive performance of both statistical and RTM-based methods and how this effect differs between the analyzed traits (Fig. 1).

2. Material and methods

2.1. Data acquisition

We obtained the trait data and plant spectra in an outdoor cultivation in the botanical garden of the Karlsruhe Institute of Technology (Karlsruhe, Germany, N49°0′45.77 E8°25′8.49). Plants were watered regularly at mean temperature of 10.5 °C. The data was acquired weekly for plants that completed the juvenile phase and that were not senescent in the years 2016 and 2017. We selected 45 herbaceous species common to Central Europe and greatly differing in plant functioning (see Appendix A). Each species was cultivated homogenously in four separate 0.4 × 0.4 m pots, each filled with 30 l standardized substrate. For further details on species selection, plant cultivation, trait measurements (Section 2.1.1), and canopy reflectance (Section 2.1.2) see also Kattenborn et al., 2019a.

2.1.1. Plant traits

We aimed for three pigment samples per pot and week. Given the vast amount of resulting individual measurements (~540 per week), common destructive pigment retrieval techniques using laboratory spectroscopy were not feasible. We thus retrieved chlorophyll *a* + b content (*Cab*, µg/cm^2), carotenoid content (*Car*, µg/cm^2), and anthocyanin content (*Ant*, µg/cm^2) by means of inversion of leaf spectra using PROSPECT-D (Féret et al., 2017) and wavelet decomposition (Blackburn, 2007). Leaf spectra were acquired with an ASD FieldSpec III spectroradiometer (Analytical Spectral Devices, Inc., Boulder, CO, USA) and leaf clip. This approach is sufficiently accurate (Kattenborn et al., 2019; Li et al., 2018) and allows analyzing large quantities of data in a

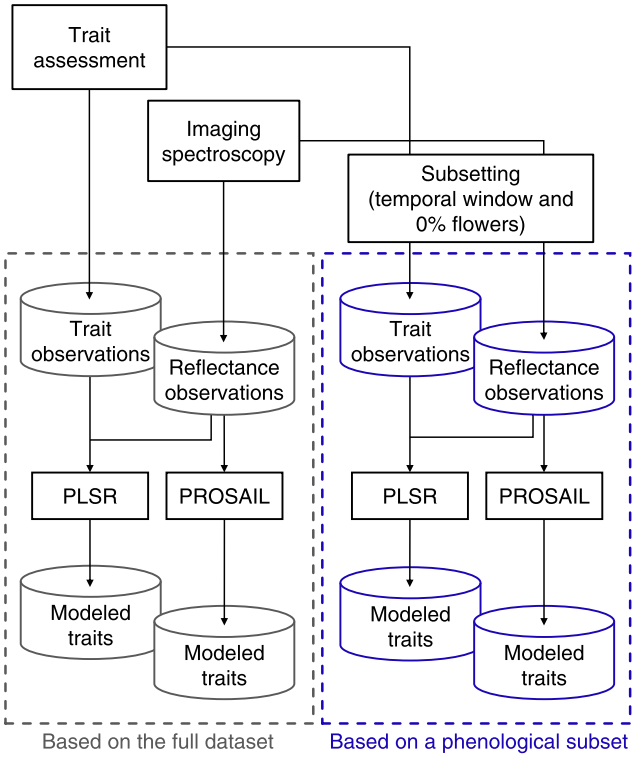

Fig. 1. Simplified representation of the study.

non-destructive way. For species with leaves smaller than the opening of the leaf clip (2 cm diameter), we seamlessly and without overlap arranged multiple leaves side by side on adhesive tape before scanning.

Leaf Area Index (*LAI,* m^2/m^2) was estimated using an Accu-PAR LP–80 ceptometer (METER Group, Inc., Pullman, USA) by averaging 18 individual readings per pot. For measurements of pigment contents and *LAI*, measurements from the four pots per species were averaged to weekly median values per species.

For the retrieval of dry matter content (*Cm*, g/cm^2) and equivalent water thickness (*Cw*, g/cm^2) we conducted measurements on species-basis instead of pot-basis to minimize destructive sampling. For these measurements, approximately 10 g of whole mature leaves without twig were plucked from all four pots. Then fresh weight was determined, and total leaf area was captured using a flatbed scanner (Canon LiDE 70). Following the protocol by Pérez-Harguindeguy et al. (2013), samples were then oven-dried and subsequently weighted. We then computed *Cm* and *Cw* using total leaf area, fresh weight, and dry weight.

Leaf constituents were scaled up to canopy-level contents (*CCab, CCar, CAnt, CCw, and CCm*) by multiplying the respective traits with *LAI*.

For parametrization of RTM-inversions, we also obtained species-specific average leaf angles (*ALA*, °) from leaf inclination distributions that we derived using leveled digital photographs and the procedure described by Ryu et al. (2010). As this procedure is very laborious, *ALA* was only retrieved once when the plants were fully developed. The area-proportional percentage of the flower and inflorescence coverage was visually estimated from nadir photographs.

Samples including small seedlings, disease-infested plants, or dead plants were excluded from further analyses resulting in a total sample size of n = 609 of paired trait-reflectance observations (onwards *full dataset*). Summary statistics of all measured variables are shown in Table 1.

2.1.2. Canopy reflectance

We measured the hyperspectral canopy reflectance using the ASD FieldSpec III (fore optic, field of view of 15°, 0.75 m above the canopy). The spectroradiometer records the solar electromagnetic radiation in 2101 spectral bands from 400 to 2500 nm. We performed measurements during bright sky conditions between 10 am and 16 pm GMT + 1. To obtain canopy reflectance, the vegetation signal was normalized using a white reference (Spectralon), which we remeasured at least every five minutes. For each pot, nine spectra were acquired at nadir angle in different positions and subsequently averaged to a mean reflectance spectrum. Removal of atmospheric water absorption bands resulted in a total of 1568 spectral bands. We removed noise by applying a first-order Savitzky-Golay filter with a frame size of 25 nm (Savitzky and Golay, 1964). The preprocessed data are available online (Kattenborn et al., 2017b).

2.2. Statistical trait retrieval

In the statistical approach, we used the widely applied PLSR algorithm, which is known to give good results on locally calibrated datasets (Asner et al., 2015; Homolová et al., 2013). PLSR reduces the dimensionality of the spectral information by decomposing them into latent variables that are linearly related to both predictors and target data. An optimum number of latent variables is then used in a linear regression (Wold et al., 2001). We performed 10-times 5-fold cross-validation for model evaluation. The final trait estimates were derived by averaging predictions of the respective validation datasets (hold-out folds) from each repetition. The number of latent variables was identified via minimal root mean squared error (RMSE) after cross-validation and was fixed in the temporal analysis. Analyses were conducted in R statistical environment (R Core Team, 2018), using packages 'pls' (Mevik et al., 2018) and 'caret' (Kuhn, 2018). We also tested Random Forest models that resulted in very similar predictions (Appendix E) and we therefore only present the results of the more parsimonious PLSR algorithm in the main manuscript.

Table 1
Summary statistics of the traits retrieved from the cultivated plants.

Measured variable	Min.	Mean	Max.	StDev	CV [%]
Chlorophyll *a* + *b* [µg/cm²]	8.14	31.74	65.58	9.98	31.4
Carotenoids [µg/cm²]	4.58	9.09	13.02	1.57	17.3
Anthocyanins [µg/cm²]	0.56	1.23	2.81	0.36	28.9
Equivalent water thickness [g/cm²]	0.004	0.015	0.058	0.007	44.4
Dry matter [g/cm²]	0.0006	0.0045	0.0118	0.0017	38.7
Leaf Area Index [m²/m²]	0.26	3.94	7.14	1.53	38.9
Average leaf angle [°]	5.08	42.91	78.68	15.86	36.9
Flower coverage [%]	0.00	5.33	70.00	9.18	1.72

StDev = Standard Deviation, CV = Coefficient of variation.

2.3. RTM-based trait retrieval

For the RTM-based trait retrieval, we chose the latest version of the PROSAIL model (Jacquemoud et al., 2009), which combines the leaf model PROSPECT-D (Féret et al., 2017; Jacquemoud and Baret, 1990) and the canopy model 4SAIL (Verhoef, 1984; Verhoef et al., 2007). In PROSPECT a leaf is considered a transparent plate with a compact layering of rough parallel surfaces resulting in isotropic scattering. PROSPECT simulates leaf reflectance and transmittance as a function of the mesophyll structure parameter (*N)* and the biochemical constituents chlorophyll *a* + b (*Cab)*, carotenoid (*Car)*, anthocyanin (*Ant)*, brown pigment (*Cbrown)*, equivalent water thickness (*Cw),* and dry matter content (*Cm)*. *N* is defined as the number of compact layers ('plates') and specifies the number of air to cell interfaces (Jacquemoud et al., 2009). *Cbrown* is a relative coefficient for brown pigments (e.g., tannins, polyphenols, other denatured proteins) accumulating during leaf senescence (Féret et al., 2008). Leaf reflectance and transmittance modeled by PROSPECT are inputs to SAIL, which inter alia models top–of–canopy reflectance. SAIL characterizes the canopy as one-dimensional turbid medium, assuming homogeneous distribution of identical, small, and flat leaves with random azimuth angles (Verhoef, 1984). Apart from leaf optical properties, SAIL requires information on *LAI*, leaf angle distribution function (Campbell, 1990), solar zenith angle (*tts)*, observer zenith angle (*tts),* relative azimuth angle (*psi)*, soil background reflectance, soil brightness (*psoil)*, diffuse radiation (*skyl*), and hot-spot size parameter *hot* (Kuusk, 1991).

Given the ill-posedness of RTM-inversions, i.e., the problem that a given reflectance could result from different combinations of trait expressions, various authors have recommended the use of prior knowledge while parameterizing RTMs (Baret and Buis, 2008; Darvishzadeh et al., 2008; Vohland and Jarmer, 2008). We selected PROSAIL input parameters (Table 2) in accordance with in situ measured traits. Moreover, information about the relationships between leaf constituents can be reasonable constraints to parameter combinations (Ali et al., 2016; Vohland et al., 2010). In our data, we observed linear correlations between *Ant* and *Cab* (Pearson's correlation r = 0.57) and *Car* and *Cab* (r = 0.89) with ratios for *Car/Cab* from 0.19 to 0.74 and *Ant/Cab* from 0.02 to 0.2. To preserve realized relationships, we coupled the corresponding parameters within the 10%- and 90%-quantile of the observed ratios (*Car/Cab*: 0.24–0.36, *Ant/Cab*: 0.028–0.051). The same procedure was applied for *Cw* and *Cm* (r = 0.42), showing ratios (*Cw/Cm*) from 1.05 to 17.0 (10%–90%–quantile: 2.04–5.74). For the soil reflectance parametrization within SAIL, we acquired pure soil reference spectra for both wet and dry soil. We fixed *psoil* at 0.5 to reduce the ill-posed problem of model inversions and considering that reflectance spectra of closed canopies are not greatly affected by soil properties.

We tested three inversion procedures: (1) lookup-table (LUT)-based inversion with RMSE as cost function (invLUT), (2) LUT-based inversion in combination with continuous wavelet transformation and RMSE as cost function ($invLUT_{wavelet}$), and (3) hybrid inversion technique using

Table 2
Parameter settings for PROSAIL for the generation of the lookup table.

Model	Parameter	Abb.	Unit	Value/Range
PROSPECT-D	Leaf structure coefficient	*N*	–	1–2
	Chlorophyll $a + b$ content	*Cab*	µg/cm^2	8–65
	Carotenoid content	*Car*	µg/cm^2	1.9–23.4[a]
	Anthocyanin content	*Ant*	µg/cm^2	0.22–3.25[a]
	Brown pigment content	*Cbrown*	–	0–0.3
	Equivalent water thickness	*Cw*	g/cm^2	0.005–0.03
	Dry matter content	*Cm*	g/cm^2	0.0008–0.014[b]
4SAIL	Leaf area index	*LAI*	m^2/m^2	0.2–7.5
	Average leaf angle	*ALA*	°	5–80
	Hot spot size	*hot*	–	0.1[c]
	Soil brightness	*psoil*	–	0.5
	Solar zenith angle	*tts*	°	Fixed at measurement
	Observer zenith angle	*tto*	°	0[c]
	Relative azimuth angle	*psi*	°	0[c]
	Diffuse radiation	*skyl*	–	Fixed at measurement

[a] Possible range after coupling with *Cab*.
[b] Possible range after coupling with *Cw*.
[c] Fixed due to nadir acquisition.

Random Forest (invHyb). Hybrid inversions are based on RTM-simulated spectra that are used to calibrate statistical models. For each method, inversion was applied on pot-level reflectance and the resulting trait estimates subsequently pooled to median species-specific values.

2.3.1. Lookup table approaches

For invLUT, a variety of possible parameter combinations is stored in a lookup table and the corresponding spectra are modeled with PROSAIL. The actual inversion is the process of identifying the modeled reflectance spectrum – and thus the underlying traits – that is closest to the measured reflectance. This is done by querying the modeled spectra and applying a cost function. For our study, the lookup table comprised 100,000 parameter combinations drawn randomly from uniform distributions. We added randomly generated noise to the simulated spectra to increase the robustness (Locherer et al., 2015). The random noise was generated from normal distribution with zero-mean and standard deviation of 0.0001.

For invLUT$_{wavelet}$, we used RMSE in combination with continuous wavelet transformation. Wavelets are simple mathematical functions that can be used to decompose reflectance spectra into frequency components at different scales. Several studies showed that wavelet analysis improved RTM-based parameter retrieval (Ali et al., 2016; Banskota et al., 2013; Blackburn and Ferwerda, 2008) as they can decouple spectral features of different traits. For instance, variation in pigments results in relatively narrow spectral features, whereas scattering processes as resulting from variation in *LAI* are rather displayed in broad spectral features. For each modeled reflectance spectrum, we calculated wavelets with a second derivative Gaussian function ('Mexican hat') at eight scales in a range from 1 to 350 nm using the R-package 'wmtsa' (Constantine and Percival, 2017). We excluded wavelets at the first two scales as they primarily represent high-frequency noise. Inversion using invLUT$_{wavelet}$ is done by identifying the modeled reflectance whose wavelets are closest to wavelets of the measured reflectance.

For invLUT and invLUT$_{wavelet}$, we selected the 100 parameter combinations resulting in the smallest RMSE. Final trait estimates were derived using weighted mean according to the RMSE values (see Vohland et al., 2010).

2.3.2. Hybrid approach

Following the implementation in previous studies (Doktor et al., 2014; Feilhauer et al., 2018, 2017) we applied the hybrid approach (invHyb) using Random Forest regression models (Breiman, 2001) that were trained on a large lookup table (n = 55,000). The ability to handle high data dimensionality and multicollinearity makes Random Forest highly suitable for hyperspectral data (Belgiu and Drăguţ, 2016). Separate Random Forest models per trait were trained with RTM-simulated spectra of 5,000 randomly selected parameter combinations. Larger sample sizes substantially increased computational time without model improvements (not shown). The remaining 50,000 parameter combinations served as validation data to assess the predictive performance (for calibration accuracies see Appendix B).

We determined accuracies of the four trait retrieval approaches using RMSE, range normalized RMSE (nRMSE), and the coefficient of determination R^2 between trait estimates and reference measurements.

2.4. Impact of phenology on trait retrievals

We analyzed the impact of phenology on PLSR- and PROSAIL-based retrieval methods in terms of two aspects: (1) we assessed how flowering affects trait retrieval accuracy, by comparing the model results on different subsets of the full dataset with increasing percentages of flowering canopies (Section 2.4.1); (2) we investigated to what extent the temporal variability affects trait retrieval accuracy, by comparing trait retrievals within the growing season using a moving window approach (Section 2.4.2).

2.4.1. Impact of flowering

For each trait, a PLSR model was calibrated with 100 randomly selected observations of non-flowering (0% flower coverage) plants. In the context of this study, flowering also comprised the presence of inflorescences, even though the plant might not yet be or not anymore be in blossom. The model was subsequently applied to 101 independent subsets including different proportions of observations that include flowers (0, 1, 2…100%). Each of these 101 subsets was created by proportionally sampling a total of 100 flowering and non-flowering observations from the original dataset (e.g., subset corresponding to 73% included 73 observations with and 27 observations without flowers). From the predictions of the subsets, we obtained model accuracies in terms of $R^2_{0–100\%}$ and $RMSE_{0–100\%}$ (from 0% to 100% flowering plants respectively). The whole procedure was repeated 100 times, resulting in 10,100 values per accuracy metric (101 different flowering percentages times 100 repetitions). With the resulting accuracies, we calculated linear regressions between observed $R^2_{0\text{-}100\%}$ ($RMSE_{0–100\%}$) against the percentage of flowering plants. We performed a similar analysis to test for the impact of flowering on the RTM-based trait retrieval that resulted in very similar findings (Appendix C).

2.4.2. Impact of temporal trait variability

To assess how the trait retrieval accuracy varies during the growing season we used a moving window along the day of growing season (DOGS). DOGS is defined as the day on which measurements were acquired, starting with day of germination. The window was applied in 21 steps, corresponding to the number of weeks in the considered growing season. We only considered observations without flowers (the specific effect of flowers is assessed in Section 2.4.1). We used DOGS instead of the day of the year for better comparability between years because dates of germination varied. For the statistical trait retrieval, we calculated PLSR models for each trait within the respective timeframe. In contrast to the PLSR models trained with cross-validation on the full dataset (Section 2.2), we here used leave-one-out cross-validation to compensate for the smaller number of observations in each temporal window. For the RTM-based methods, we calculated linear regressions between the selected measurements and the corresponding estimates in the temporal window. We set the window size to 56 days to ensure a large

enough sample size in each temporal window ($53 < n < 176$). Based on the temporal patterns, we qualitatively chose the timeframe with highest model accuracies – in terms of R^2 and RMSE – and kept those observations in the *phenological subset*.

3. Results

3.1. Impact of flowering

An increasing percentage of flowering plants decreased the predictive performance of PLSR models for five traits, except for *Cw,* which showed no trend (all significant at $p < 0.001$, Fig. 2). The assessment of *Car* was most affected by flowering (Fig. 2, $R2 = 0.61$ between retrieval accuracy and the fraction of flowering canopies), with a decrease in model fit from an initial $R^2_{0\%} = 0.58$ (mean R^2 of the 100 repetitions at 0% flowering) to $R^2_{100\%} = 0.25$ (mean R^2 of the 100 repetitions at 100% flowering). A slightly weaker effect was found for models of *Cab* ($R^2 = 0.5$) with a decrease in model fit from $R^2_{0\%} = 0.57$ to $R^2_{100\%} = 0.31$. *Ant* and *Cm* showed similar results with $R^2 = 0.3$ and a decrease in model fit from $R^2_{0\%} = 0.4$ to $R^2_{100\%} = 0.2$. The negative impact of flowering on the predictive performance was smallest for *LAI* ($R^2 = 0.06$, $R^2_{0\%} = 0.33$, $R^2_{100\%} = 0.26$). The influence of flowering on model accuracy for canopy-level contents as well as the influence on model RMSE is given in Appendix C. The findings from the RTM-based analyses showed the same overall trends and can also be found in Appendix C.

3.2. Ideal temporal window

For all three RTM-based approaches, *Cab* and *Car* were best retrieved towards senescence, whereas *LAI* and *Cw* tended towards the first half of the growing season (Fig. 3a). For *Ant* and *Cm,* timing showed only a small influence on trait retrieval. On canopy-level, retrieval accuracies largely followed the temporal patterns of *LAI*. For PLSR models, seasonal differences were smaller. Except for *Cm* and *LAI,* we found no strong temporal patterns. The accuracy of *LAI* retrieval decreased towards senescence, whereas for *Cm* accuracy increased.

3.3. Full dataset

Measured traits and traits predicted through PLSR modeling showed R^2-values between 0.22 and 0.49 with slope values between 0.24 and 0.5 and nRMSE below 0.17 (Fig. 4a–5a). Strongest correlations between modeled and measured traits were observed for *Cab* ($R^2 = 0.49$) and *Car* ($R^2 = 0.47$) at leaf-level and *CCab* ($R^2 = 0.42$) at canopy-level. *Cm* ($R^2 = 0.22$) showed the weakest correlations.

InvLUT (Fig. 4b–5b) yielded considerably lower model fits and higher nRMSE for most traits. Best results were obtained for pigments with the highest correlation for *Cab* ($R^2 = 0.41$). *LAI* was the most difficult trait to estimate using invLUT indicated by nRMSE = 0.3 and a low correlation between modeled and measured trait values ($R^2 = 0.03$). For canopy-level contents, *CCw* was best modeled ($R^2 = 0.28$).

$InvLUT_{wavelet}$ (Fig. 4c–5c) introduced minor improvements and resulted in slightly smaller nRMSE and higher R^2 than invLUT.

The large variations in the modeled trait ranges of both lookup table-based approaches were also apparent in the results of invHyb (Fig. 4d–5d). Especially for leaf pigments, a clear systematic underestimation of trait values could be observed here, given that most observations lie below the 1:1-line. Best results were obtained for *Cab* with $R^2 = 0.3$ and nRMSE = 0.31.

3.4. Phenological subset

Model accuracies on the phenological subset (observations with flowers removed and based on the temporal window selection) clearly differed from results of the full dataset (Figs. 4 and 5, grey dots vs. blue triangles). Except for *Cw* and *CCm*, all PLSR models showed an increase

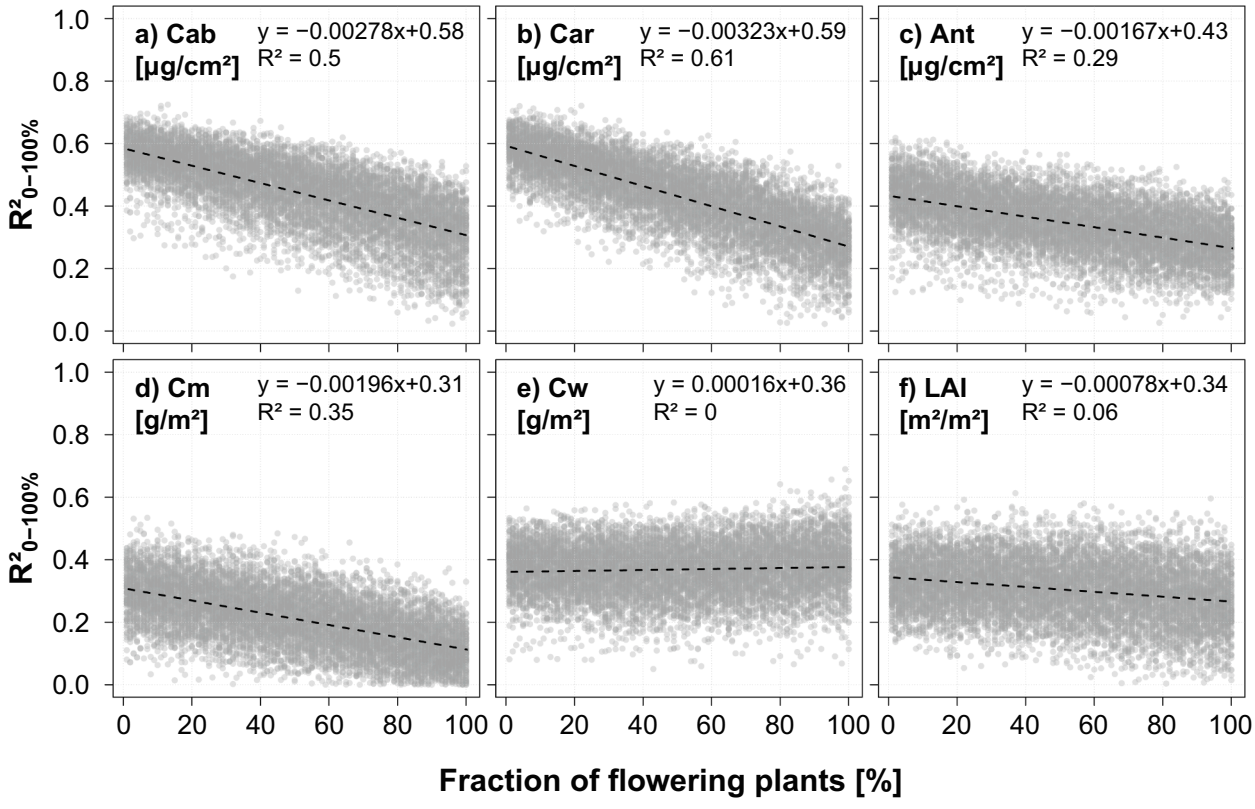

Fig. 2. Coefficient of determination of the PLSR models for the leaf-level variables and *LAI* in dependency of the fraction of flowering plants. The results for the canopy-level leaf constituents are given in Appendix C.

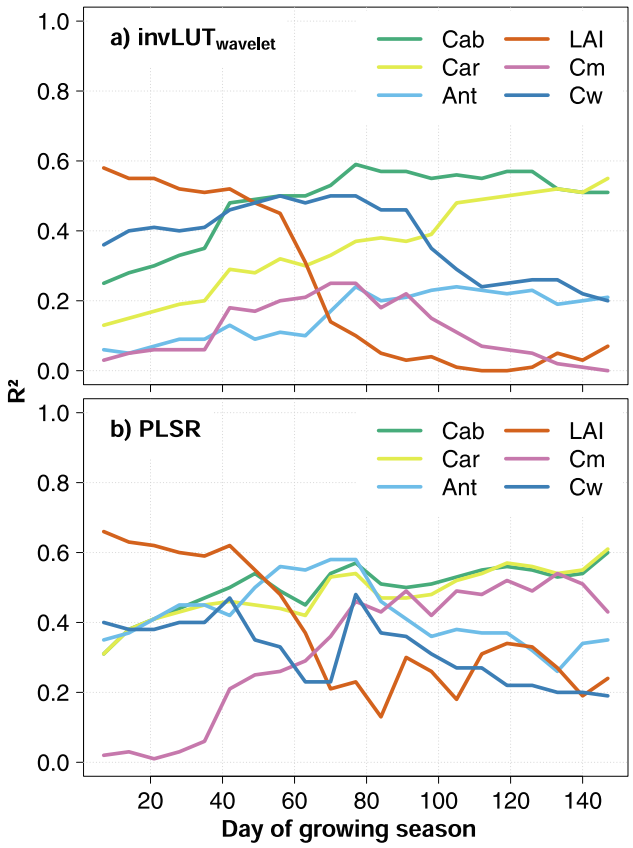

Fig. 3. Temporal variations of the coefficient of determination along the day of growing season exemplary for a) invLUT$_{wavelet}$ and b) PLSR. The temporal variation of the remaining models is available in Appendix D.

in model fit with highest accuracy for *CCab* (up to $R^2 = 0.7$). Slope values only slightly improved with lowest values m = 0.2 for *CCm* and highest m = 0.68 for *Car*. All PLSR models were biased to the effect that lower values were overestimated and higher values were underestimated. This resulted in poorly represented trait ranges especially for *Cm, Cw,* and *CAnt*.

Compared to the full dataset, both invLUT and invLUT$_{wavelet}$ showed better model accuracies when applied to the phenological subset, with better results for invLUT$_{wavelet}$. For *Cab*, *Car*, *LAI,* and canopy-level contents, slope values closer to m = 1 indicate that lookup table-inversions worked equally well throughout the entire trait ranges. *LAI* showed largest improvements in model accuracies on the phenological subset (invLUT: $R^2 = 0.47$, invLUT$_{wavelet}$: $R^2 = 0.52$).

The results of invHyb applied on the phenological subset resulted again in underestimation of leaf pigment contents, and only improvements in terms of R^2 could be observed but not for the slope values. Less underestimation was observed for leaf pigments up-scaled to canopy-level (e.g., *CCab*; cf. Figs. 4d vs. 5d), which, however, was mainly due to better *LAI* predictions.

4. Discussion

4.1. Flower coverage limits retrieval of functional traits

The distinct spectral signal of flowers has been discussed as a good indicator for the remote discrimination of species (Andrew and Ustin, 2008; Ge et al., 2006; He et al., 2011; Kattenborn et al., 2019) or pollination types (Feilhauer et al., 2016). Contrasting, our results show that flowering has a negative impact on the predictive performance of statistical and RTM-based methods for estimating leaf and canopy traits (except for *Cw*). The negative effect of flowering on retrieval accuracies can be explained as the presence of inflorescence has consequences throughout the optical spectrum (Landmann et al., 2019) hampering the assessment of any trait from canopy reflectance data. The largest influence was found for leaf pigments *Cab* and *Car*, probably because their characteristic absorption features largely overlap with the spectral features of flowers that are naturally prominent in the visible domain (Chen et al., 2009; Kevan et al., 1996). The retrieval of traits with broad absorption and scattering features, like *LAI*, *Cm,* and *Cw* is less affected.

4.2. Retrieval accuracies vary during the growing season

Results from the moving window approach analyzing temporal changes in trait retrieval are unlikely to be transferable across species, years, and geographic locations but shed light on the variability in time. The results show that trait retrieval does not perform equally well within the growing season. Temporal differences were larger for PROSAIL-based methods than for PLSR. We assume that the application of PROSAIL is most successful when canopy conditions are closest to the model assumptions. This explains why several traits are better estimated towards the center or end of the growing season (except for *LAI* as discussed below), where the plant canopies were fully developed and corresponded most to a turbid medium (a primary assumption of PROSAIL). Statistical methods can better compensate for seasonal variation given that respective observations are included in the training stage.

Leaf-level pigment contents were better retrieved towards the end of the growing season, which could result from accumulating *LAI* and thus overall higher total pigment content, which in turn results in increased light absorption and thus in a more distinct spectral response. Besides, increased range of pigment contents towards the end of the growing season might have caused a better model fit. *LAI* featured an opposing trend and was better retrieved at the beginning. This can be explained as dense canopies suffer from saturation effects for *LAI* retrieval and could result in larger errors for higher *LAI* values that were especially present towards the end of the growing season.

Given the above-mentioned explanations, temporal trends of the canopy-level traits, e.g., *CCab* (*Cab* * *LAI*) largely followed the dynamics observed in *LAI* and accuracies dropped to a minimum at the end of the growing season. *Cab* and *Car*, were best retrieved towards the end of the growing season, whereas the corresponding canopy-level variables, *CCab* and *CCar*, had their temporal optimum for trait retrieval at the beginning of the growing season. This underlines the key role of *LAI* for the estimation of canopy-level contents as has been reported in previous studies (e.g., Sehgal et al., 2016; Vohland and Jarmer, 2008).

4.3. Model performance per trait

Our dataset includes a wide range of optically relevant plant traits and covers a large part of a plants' lifecycles. Other studies have mostly investigated limited timeframes and numbers of traits, which hampers comparison with our results. To facilitate a comparison we focused on results from the phenological subset.

Cab was best retrieved with invLUT$_{wavelet}$. The model accuracy ($R^2 = 0.59$, nRMSE = 0.15) is well in line with expected retrieval accuracies (nRMSE of 0.214) for physically-based approaches as reported in the review by van Cleemput et al. (2018). Darvishzadeh et al. (2008) have also used a LUT-approach and found an overall comparable error rate (RMSE = 6.8 μg/cm^2) but a low proportion of explained variation ($R^2 = 0.27$). In our study, PLSR gave the best linear fit for *Car* and *Ant* but the established relationships are rather biased. With a similar model fit but with slope values closest to 1, invLUT$_{wavelet}$ resulted in better overall retrieval performance. Model accuracies for *Car* and *Ant* differed largely between PLSR and RTM-based methods, with higher model accuracies for PLSR. Given the strong correlation between *Car, Cab,* and *Ant*, respectively, values of *Ant* and *Car* might have been an indirect expression of the better visible *Cab*. This is supported by the fact that RTM-based methods were not able to disentangle the subtle spectral

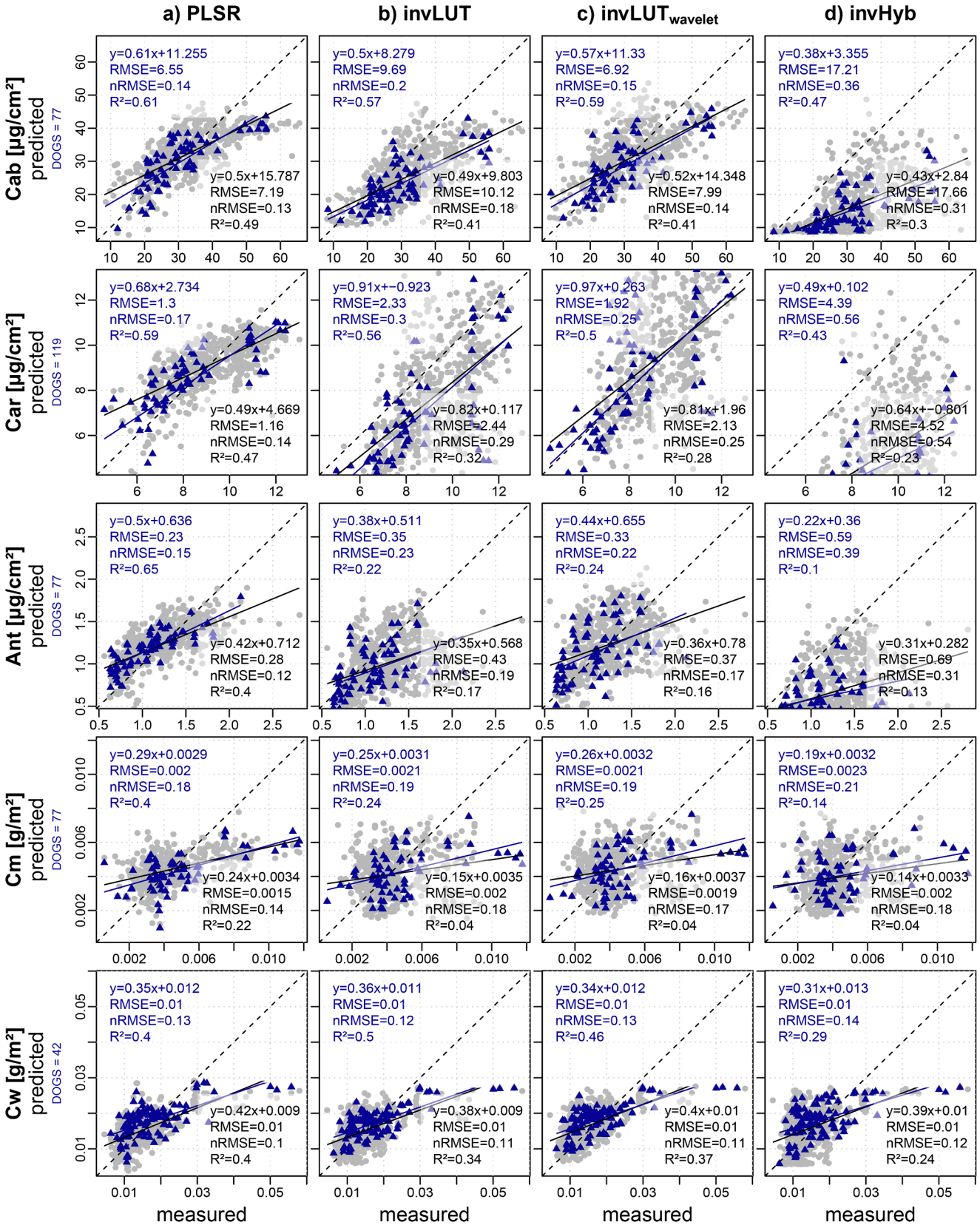

Fig. 4. Predicted versus measured chlorophyll (*Cab*), carotenoid (*Car*), anthocyanin (*Ant*), leaf dry matter (*Cm*), and leaf water content (*Cw*) from (a) PLSR models, (b) invLUT-, (c) invLUT$_{wavelet}$-, and (d) invHyb-inversion. Results on the full dataset are shown in grey and results on the phenological subset are superimposed as blue triangles. DOGS stands for the center day of the temporal window. (For interpretation of the references to color in this figure legend, the reader is referred to the web version of this article.)

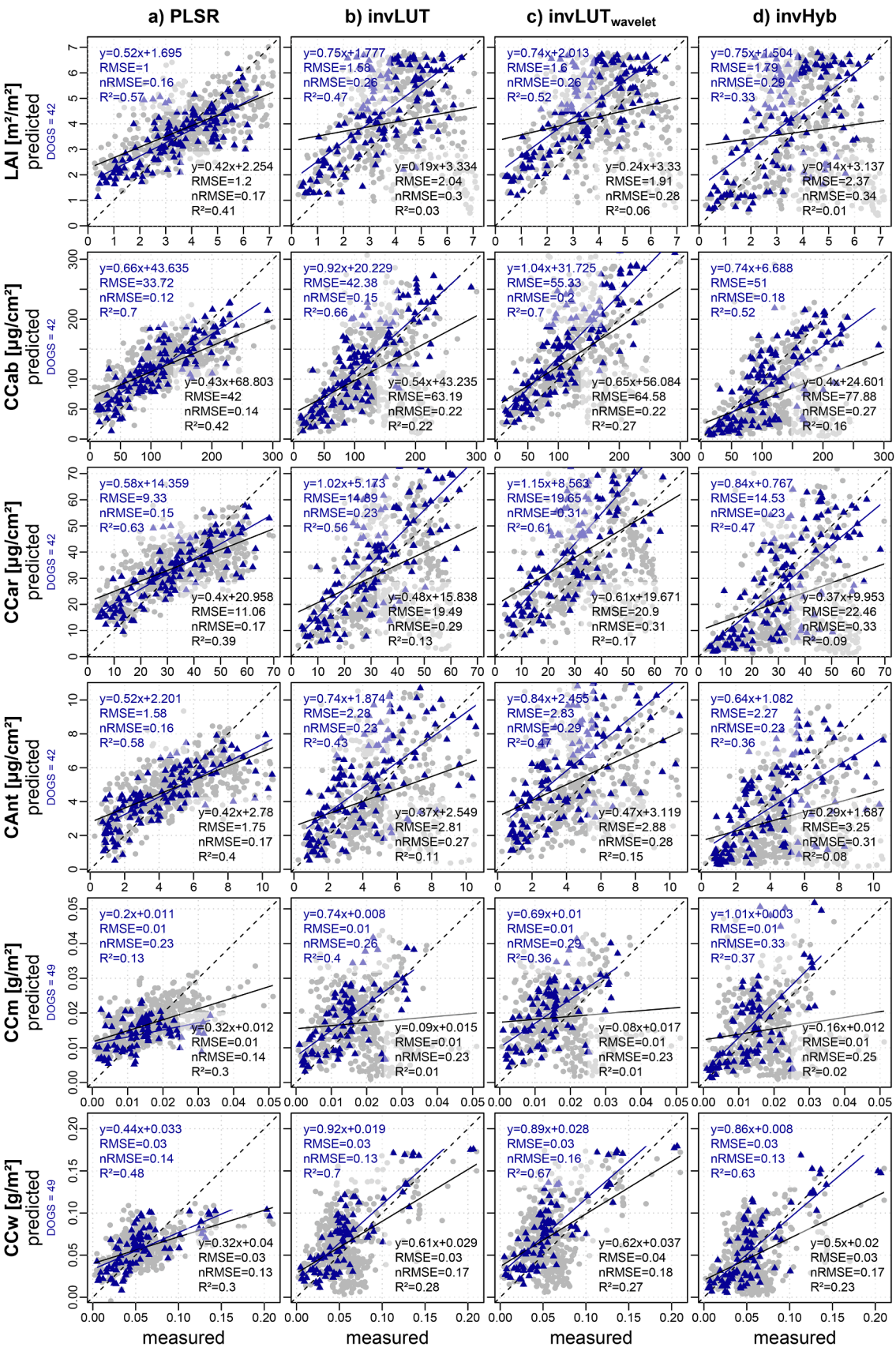

Fig. 5. Predicted versus measured canopy-level contents of Leaf Area Index (*LAI*), chlorophyll (*CCab*), carotenoid (*CCar*), anthocyanin (*CAnt*), dry matter (*CCm*), and water content (*CCw*) from (a) PLSR models, b) invLUT-, (c) invLUT$_{wavelet}$-, and (d) invHyb-inversion. Results on the full dataset are shown in grey and results on the phenological subset are superimposed as blue triangles. DOGS stands for the center day of the temporal window. (For interpretation of the references to color in this figure legend, the reader is referred to the web version of this article.)

response of *Ant* and *Car*. This is not to say that *Ant* and *Car* are generally not retrievable from RTM-inversions. For example, Zarco-Tejada et al. (2018) have used *Ant* retrievals from PROSAIL-inversions of airborne hyperspectral data to detect the plant disease *Xylella fastidiosa* in olive trees. Yet, they targeted monocultures and therefore the absorption features of *Ant* might have been better visible than in datasets that include several species with a greater variation of traits expressions. Additionally, monocultures feature a comparable small range of trait expressions, which in turn enables to further restrict the trait ranges (e.g., in a lookup table) and thus the ill-posed problem.

For *LAI*, PLSR was slightly better in terms of R^2 and RMSE but slope values were again best for $invLUT_{wavelet}$. A variety of studies have reported higher accuracies for RTM-based *LAI* retrieval than in our study, e.g., Atzberger et al. (2013) with $R^2 = 0.91$ and RMSE = 0.53 for grassland and Jay et al. (2017) with $R^2 = 0.81$ and RMSE = 0.39 for a range of crops. However, difference in accuracies between these and our studies can be easily explained by the wide plant functional gradient represented in our dataset (cf. Kattenborn et al., 2019a), magnifying the already inherent ill-posed problem of the RTM-based trait retrievals. Only a few studies have reported lower accuracies (e.g., Botha et al., 2007: $R^2 = 0.13$, RMSE = 0.97).

A commonality of all four retrieval methods is that estimation of leaf constituents was more accurate when scaled up to the canopy-level using *LAI*. This is in line with the findings from previous studies (Darvishzadeh et al., 2008; Jay et al., 2017; Roelofsen et al., 2013; Sehgal et al., 2016; Vohland and Jarmer, 2008) and is especially applicable to *Cm* and *Cw*, showing very weak relationships on leaf-level but highest accuracies on canopy-level. This is because not only functional traits itself but also their interactions contribute to the spectral variation (Jacquemoud et al., 2009). For canopy-level contents, *LAI* acts as a multiplier of the absorption by the respective constituent and their joint effect is much easier modeled than the decoupled effects by themselves. The best retrieval method for canopy-level contents was $invLUT_{wavelet}$. As for *LAI* retrieval, Vohland et al. (2010) have reported higher model accuracies for *CCm* ($R^2 = 0.72$, RMSE = 0.002 μg/cm^2) and *CCw* ($R^2 = 0.83$, RMSE = 0.0078 μg/cm^2), which again may be explained by the complexity of the present data. Darvishzadeh et al. (2008) and Jay et al. (2017) have reported similar accuracies for the retrieval of *CCab* ($R^2 \geq 0.7$, RMSE $\leq$ 22 μg/cm^2).

4.4. Comparison of trait retrieval methods

As elaborated in the methods section, the reference measurements for *Cab*, *Car*, and *Ant* were also derived using spectroscopic measurements and the leaf-level RTM PROSPECT. Therefore, a direct comparison of model accuracies between the inversions of the canopy-RTM PROSAIL and PLSR could be biased. However, the spectra for the reference data retrieval were taken independently at leaf-level using a plant probe (leaf clip). Also, the resulting differences between models found for the respective traits were in line with the trends for *LAI*, *Cm*, and *Cw* that were measured directly.

In comparison to trait retrieval from the full dataset, predictive performances of all retrieval methods clearly improved with the phenological subset. This shows that both statistical models and RTMs were affected by phenology. As can be seen in the large variations of the scatterplots (Figs. 4 and 5, grey dots), it is obvious that for some observations RTM-based methods were very inaccurate. This might result from the ill-posedness, which is inherent with RTM-based methods and originates from the problem that multiple parameter combinations may generate very similar spectral reflectance (Combal et al., 2003). Alternatively, such inaccuracies can be caused by the fact that the respective canopies did not meet the model assumptions of PROSAIL (e.g., leaf clumping, heterogeneous distribution of leaves with different constituents). Although PLSR models yielded the highest model accuracies in terms of R^2, they often resulted in biased predictions of trait expressions. A possible reason might be an overall bad predictive performance due to a lack of a corresponding signal in the reflectance data. Furthermore, we suspected insufficient capacity of PLSR to deal with non-linearity in the relationship between traits and reflectance. Although PLSR is a widely used method and known to be quite flexible in this regard, it is still a linear model that sometimes fails to project the nonlinearities using – even numerous – latent vectors (Kiala et al., 2016). However, a comparative analysis using non-parametric Random Forest algorithm (Appendix E) revealed almost identical patterns, suggesting the bias in predictions not being caused by the statistical algorithm itself.

The performance of PROSAIL-based trait retrieval methods on the phenological subset was generally in the order invHyb < invLUT < $invLUT_{wavelet}$. The hybrid model systematically underestimated the trait expressions and had the largest deviances. We thus consider invHyb as the least suited approach. invLUT was more accurate in terms of R^2 and RMSE and showed a lower bias. The fact that invLUT performed better than invHyb is in line with Vohland et al.(2010), who have tested different inversion techniques for trait retrieval of summer barley using PROSAIL and HyMap data and found lookup table-inversion to outperform hybrid-inversion with artificial neural networks. $invLUT_{wavelet}$ provided the best results since it was able to disentangle spectral features, e.g., broad features that originate from scattering (e.g., by *LAI*) and narrower absorption features of leaf constituents (pigments, water, and dry matter). This is in line with previous studies that have demonstrated the value of continuous wavelet transformation for the inversion of PROSPECT (Blackburn and Ferwerda, 2008; Li et al., 2018). Likewise, Banskota et al. (2013) showed the potential of discrete wavelet transformations for *LAI* retrieval from airborne hyperspectral data through inversion of the Discrete Anisotropy Radiative Transfer model.

4.5. Limitations and outlook

With the experimental setup of cultivated plants, including repetitions per species and repeated measurements, we aimed to acquire robust and ample in situ data and to avoid external effects as much as possible. For logistical reasons, measurements were performed covering two growing seasons in 2016 and 2017 and were joined on one 365 days-axis with their respective day of growing season. Since only large-scale temporal trends were analyzed we assume minor phenological differences to be negligible.

The effect of flowers was assessed in a binary mode, where trait retrievals for flowering and non-flowering plants were compared to trait retrievals of exclusively non-flowering plants. We did not assess qualitative differences in flowers (e.g., petal size, color) or the quantitative differences in flower cover in the plant canopy. These aspects would require different or extended data acquisitions that could be realized in future experiments.

Based on the large number of studied species and the wide functional gradients covered, we found that RTM-based trait retrieval is not as accurate and transferable as suggested by previous studies. We assume that this relates to effects of different and often complex canopy structures of the studied species. In contrast to the assumptions in SAIL, such as homogeneous distribution of foliage, leaves of the studied plants were often heterogeneously distributed in the canopy and some plants additionally tended to leaf clumping. Pronounced leaf clumping was observed for tussock-forming grasses (e.g., *Festuca ovina, Deschampsia cespitosa*) as their leaves are all attached to the center of the plant. Another assumption in PROSAIL is Lambertian reflectance, which does not hold for species with a pronounced cuticle and corresponding wax-layers resulting in anisotropic scattering (e.g., *Cirsium acaule, Brachypodium sylvaticum*).

A fundamental limitation of reflectance-based trait retrieval originates in the reflectance measurement itself. Canopy reflectance is typically a 2D measurement, which can obviously not precisely depict (often anisotropic) 3D radiative transfer processes and structures within a plant canopy. Additionally, the influence of confounding variables, such as soil properties and diffuse radiation, might blur the causal relationship

between spectral reflectance and the traits of interest. Baret and Buis (2008) have referred to this as the forward (or direct) problem. Hence, not only different RTM-simulations can result in similar canopy reflectance but also real-world canopies can result in similar reflectance by different combinations of leaf properties, canopy structure, and illumination properties. This issue not only affects RTM-inversions but also statistical approaches. It can be assumed that retrieval of plant traits using canopy reflectance can be improved by increasing the dimensionality using multi-angular reflectance observations (see, e.g., Roosjen et al., 2018; Zhu et al., 2019). Accordingly, multi-angular earth observation data – such as acquired from platforms with across-track pointing capabilities (e.g., EnMAP) – will pave new avenues for the assessment of plant functional diversity.

Despite these limitations, the fact remains that RTMs allow for a closer approximation of the physical processes of plant-light interactions based on numerous variables. RTM-inversions are hence suited to improve our knowledge about the role of plant functional traits for remote sensing. Moreover, no calibration data are needed with RTMs, which eases applicability. With the upcoming hyperspectral satellite missions, e.g., EnMAP (Stuffler et al., 2007), PRISMA (Labate et al., 2009), or HyspIRI (Roberts et al., 2012), we thus expect the inversion of RTMs to play a key role in assessing plant traits at multiple scales. Because it is in many cases without alternative (due to a lack of suitable calibration data) spaceborne trait retrievals using RTM-inversions are suggested to be a valuable tool for mapping functional diversity and Essential Biodiversity Variables as proposed by the Group on Earth Observations Biodiversity Observation Network (Pereira et al., 2013; Skidmore et al., 2015).

5. Conclusion

We investigated how plant phenology affects the retrieval of plant functional traits from canopy reflectance using both statistical (PLSR) and physically-based modeling (multiple inversion techniques of PROSAIL RTM). Our results reveal that:

- Both approaches were largely affected by phenology in terms of temporal trait variability and by flowers in particular.
- The directionality of this effect, however, depends on the selected timeframe. The best timing for functional trait mapping regarding phenology hence depends on the studied species and functional traits. Further research on how flower coverage affects the retrieval of plant functional traits is required to improve the estimation of functional traits from canopy reflectance.
- Not only physically-based approaches, which can only decipher seasonal effects on implemented traits, struggled with phenology but also statistical approaches, which in theory can account for seasonal variation through appropriate reference data selection.
- Models were better for leaf constituents that were scaled up to the canopy-level using *LAI,* while leaf-level constituents were more difficult to retrieve. This emphasizes the importance of trait interactions and structural information to spectral variation.

CRediT authorship contribution statement

Felix Schiefer: Formal analysis, Data curation, Methodology, Software, Validation, Visualization, Writing - original draft, Writing - review & editing. **Sebastian Schmidtlein:** Funding acquisition, Methodology, Project administration, Resources, Validation, Writing - review & editing. **Teja Kattenborn:** Conceptualization, Data curation, Investigation, Methodology, Project administration, Software, Supervision, Validation, Writing - original draft, Writing - review & editing.

Declaration of Competing Interest

The authors declare that they have no known competing financial interests or personal relationships that could have appeared to influence the work reported in this paper.

Acknowledgements

This study was funded by the German Aerospace Centre (DLR) on behalf of the Federal Ministry of Economics and Technology (BMWi), FKZ 50 EE 1347. We would like to thank the employees of the botanical garden of the Karlsruhe Institute of Technology (KIT) for their generous support.

Appendix A. Supplementary data

Supplementary data to this article can be found online at https://doi.org/10.1016/j.ecolind.2020.107062.

References

Ali, A.M., Skidmore, A.K., Darvishzadeh, R., van Duren, I., Holzwarth, S., Mueller, J., 2016. Retrieval of forest leaf functional traits from HySpex imagery using radiative transfer models and continuous wavelet analysis. ISPRS J. Photogramm. Remote Sens. 122, 68–80.

Andrew, M., Ustin, S., 2008. The role of environmental context in mapping invasive plants with hyperspectral image data. Remote Sens. Environ. 112 (12), 4301–4317.

Asner, G.P., Martin, R.E., Anderson, C.B., Knapp, D.E., 2015. Quantifying forest canopy traits: Imaging spectroscopy versus field survey. Remote Sens. Environ. 158, 15–27.

Atzberger, C., Darvishzadeh, R., Schlerf, M., Le Maire, G., 2013. Suitability and adaptation of PROSAIL radiative transfer model for hyperspectral grassland studies. Remote Sens. Lett. 4 (1), 55–64.

Banskota, A., Wynne, R.H., Thomas, V.A., Serbin, S.P., Kayastha, N., Gastellu-Etchegorry, J.P., Townsend, P.A., 2013. Investigating the utility of wavelet transforms for inverting a 3-D radiative transfer model using hyperspectral data to retrieve forest LAI. Remote Sens 5, 2639–2659.

Baret, F., Buis, S., 2008. Estimating canopy characteristics from remote sensing observations: Review of methods and associated problems. Adv. Land Remote Sens. https://doi.org/10.1007/978-1-4020-6450-0.

Belgiu, M., Drăguţ, L., 2016. Random forest in remote sensing: A review of applications and future directions. ISPRS J. Photogramm. Remote Sens. 114, 24–31.

Blackburn, G.A., 2007. Wavelet decomposition of hyperspectral data: A novel approach to quantifying pigment concentrations in vegetation. Int. J. Remote Sens. 28 (12), 2831–2855.

Blackburn, G., Ferwerda, J., 2008. Retrieval of chlorophyll concentration from leaf reflectance spectra using wavelet analysis. Remote Sens. Environ. 112 (4), 1614–1632.

Breiman, L., 2001. Random forests. Mach. Learn. 45, 5–32. https://doi.org/10.1023/A:1010933404324.

Butler, E.E., Datta, A., Flores-Moreno, H., Chen, M., Wythers, K.R., Fazayeli, F., Banerjee, A., Atkin, O.K., Kattge, J., Amiaud, B., Blonder, B., Boenisch, G., Bond-Lamberty, B., Brown, K.A., Byun, C., Campetella, G., Cerabolini, B.E.L., Cornelissen, J.H.C., Craine, J.M., Craven, D., de Vries, F.T., Díaz, S., Domingues, T. F., Forey, E., González-Melo, A., Gross, N., Han, W., Hattingh, W.N., Hickler, T., Jansen, S., Kramer, K., Kraft, N.J.B., Kurokawa, H., Laughlin, D.C., Meir, P., Minden, V., Niinemets, Ü., Onoda, Y., Peñuelas, J., Read, Q., Sack, L., Schamp, B., Soudzilovskaia, N.A., Spasojevic, M.J., Sosinski, E., Thornton, P.E., Valladares, F., Van Bodegom, P.M., Williams, M., Wirth, C., Reich, P.B., Schlesinger, W.H., 2017. Mapping local and global variability in plant trait distributions. Proc. Natl. Acad. Sci. U. S. A. 114, E10937–E10946. https://doi.org/10.1073/pnas.1708984114.

Campbell, G.S., 1990. Derivation of an angle density function for canopies with ellipsoidal leaf angle distributions. Agric. For. Meteorol. 49 (3), 173–176.

Chen, J., Shen, M., Zhu, X., Tang, Y., 2009. Indicator of flower status derived from in situ hyperspectral measurement in an alpine meadow on the Tibetan Plateau. Ecol. Ind. 9 (4), 818–823.

Combal, B., Baret, F., Weiss, M., Trubuil, A., Macé, D., Pragnère, A., Myneni, R., Knyazikhin, Y., Wang, L., 2003. Retrieval of canopy biophysical variables from bidirectional reflectance. Remote Sens. Environ. 84 (1), 1–15.

Constantine, W., Percival, D., 2017. wmtsa: Wavelet methods for time series analysis. R Packag. Version 2.0-3.

Danner, M., Berger, K., Wocher, M., Mauser, W., Hank, T.B., 2017. Retrieval of biophysical crop variables from multi-angular canopy spectroscopy. Remote Sens. 9, 726. https://doi.org/10.3390/rs9070726.

Darvishzadeh, R., Skidmore, A., Schlerf, M., Atzberger, C., 2008. Inversion of a radiative transfer model for estimating vegetation LAI and chlorophyll in a heterogeneous grassland. Remote Sens. Environ. 112 (5), 2592–2604.

Díaz, S., Kattge, J., Cornelissen, J.H.C., Wright, I.J., Lavorel, S., Dray, S., Reu, B., Kleyer, M., Wirth, C., Colin Prentice, I., Garnier, E., Bönisch, G., Westoby, M., Poorter, H., Reich, P.B., Moles, A.T., Dickie, J., Gillison, A.N., Zanne, A.E., Chave, J., Joseph Wright, S., Sheremet'ev, S.N., Jactel, H., Baraloto, C., Cerabolini, B., Pierce, S., Shipley, B., Kirkup, D., Casanoves, F., Joswig, J.S., Günther, A., Falczuk, V., Rüger, N., Mahecha, M.D., Gorné, L.D., 2016. The global spectrum of plant form and function. Nature 529 (7585), 167–171.

Doktor, D., Lausch, A., Spengler, D., Thurner, M., 2014. Extraction of plant physiological status from hyperspectral signatures using machine learning methods. Remote Sens 6, 12247–12274.
Duveiller, G., Weiss, M., Baret, F., Defourny, P., 2011. Retrieving wheat Green Area Index during the growing season from optical time series measurements based on neural network radiative transfer inversion. Remote Sens. Environ. 115 (3), 887–896.
Feilhauer, H., Doktor, D., Schmidtlein, S., Skidmore, A.K., Prinzing, A., 2016. Mapping pollination types with remote sensing. J. Veg. Sci. 27 (5), 999–1011.
Feilhauer, H., Schmid, T., Faude, U., Sánchez-Carrillo, S., Cirujano, S., 2018. Are remotely sensed traits suitable for ecological analysis? A case study of long-term drought effects on leaf mass per area of wetland vegetation. Ecol. Ind. 88, 232–240.
Feilhauer, H., Schmidtlein, S., 2011. On variable relations between vegetation patterns and canopy reflectance. Ecol. Inf. 6 (2), 83–92.
Feilhauer, H., Somers, B., van der Linden, S., 2017. Optical trait indicators for remote sensing of plant species composition: Predictive power and seasonal variability. Ecol. Ind. 73, 825–833.
Feret, J.-B., François, C., Asner, G.P., Gitelson, A.A., Martin, R.E., Bidel, L.P.R., Ustin, S. L., le Maire, G., Jacquemoud, S., 2008. PROSPECT-4 and 5: Advances in the leaf optical properties model separating photosynthetic pigments. Remote Sens. Environ. 112 (6), 3030–3043.
Féret, J.-B., Gitelson, A.A., Noble, S.D., Jacquemoud, S., 2017. PROSPECT-D: Towards modeling leaf optical properties through a complete lifecycle. Remote Sens. Environ. 193, 204–215.
Ge, S., Everitt, J., Carruthers, R., Gong, P., Anderson, G., 2006. Hyperspectral characteristics of canopy components and structure for phenological assessment of an invasive weed. Environ Monit Assess 120 (1-3), 109–126.
He, K.S., Rocchini, D., Neteler, M., Nagendra, H., 2011. Benefits of hyperspectral remote sensing for tracking plant invasions. Divers. Distrib 17, 381–392.
Homolová, L., Malenovský, Z., Clevers, J.G.P.W., García-Santos, G., Schaepman, M.E., 2013. Review of optical-based remote sensing for plant trait mapping. Ecol. Complexity 15, 1–16.
Jacquemoud, S., Baret, F., 1990. PROSPECT: A model of leaf optical properties spectra. Remote Sens. Environ. 34 (2), 75–91.
Jacquemoud, S., Verhoef, W., Baret, F., Bacour, C., Zarco-Tejada, P.J., Asner, G.P., François, C., Ustin, S.L., 2009. PROSPECT+SAIL models: A review of use for vegetation characterization. Remote Sens. Environ. 113, S56–S66.
Jay, S., Maupas, F., Bendoula, R., Gorretta, N., 2017. Retrieving LAI, chlorophyll and nitrogen contents in sugar beet crops from multi-angular optical remote sensing: Comparison of vegetation indices and PROSAIL inversion for field phenotyping. Field Crops Res. 210, 33–46.
Jetz, W., Cavender-Bares, J., Pavlick, R., Schimel, D., Davis, F.W., Asner, G.P., Guralnick, R., Kattge, J., Latimer, A.M., Moorcroft, P., Schaepman, M.E., Schildhauer, M.P., Schneider, F.D., Schrodt, F., Stahl, U., Ustin, S.L., 2016. Monitoring plant functional diversity from space. Nat. Plants 2 (3). https://doi.org/10.1038/nplants.2016.24.
Kant, I., 1783. Prolegomena zu einer jeden künftigen Metaphysik, die als Wissenschaft wird auftreten können. Riga.
Kattenborn, T., Fassnacht, F.E., Pierce, S., Lopatin, J., Grime, J.P., Schmidtlein, S., Paruelo, J., 2017a. Linking plant strategies and plant traits derived by radiative transfer modelling. J. Veg. Sci. 28 (4), 717–727.
Kattenborn, T., Schiefer, F., Schmidtlein, S., 2017b. Canopy reflectance plant functional gradient IFGG/KIT. EcoSIS. https://doi.org/10.21232/krt4-6x67.
Kattenborn, T., Fassnacht, F.E., Schmidtlein, S., Nagendra, H., He, K., 2019a. Differentiating plant functional types using reflectance: Which traits make the difference? Remote Sens. Ecol. Conserv. 5 (1), 5–19.
Kattenborn, T., Lopatin, J., Förster, M., Braun, A.C., Fassnacht, F.E., 2019b. UAV data as alternative to field sampling to map woody invasive species based on combined Sentinel-1 and Sentinel-2 data. Remote Sens. Environ. 227, 61–73.
Kattenborn, T., Schmidtlein, S., 2019. Radiative transfer modelling reveals why canopy reflectance follows function. Sci. Rep. 9, 1–10. https://doi.org/10.1038/s41598-019-43011-1.
Kevan, P., Giurfa, M., Chittka, L., 1996. Why are there so many and so few white flowers? Trends Plant Sci. 1 (8), 252. https://doi.org/10.1016/1360-1385(96)20008-1.
Kiala, Z., Odindi, J., Mutanga, O., Peerbhay, K., 2016. Comparison of partial least squares and support vector regressions for predicting leaf area index on a tropical grassland using hyperspectral data. J. Appl. Remote Sens 10 (3), 036015. https://doi.org/10.1117/1.JRS.10.036015.
Kuhn, M., 2018. caret: Classification and Regression Training. R Packag. version 6.0-81 https//CRAN.R-project.org/package=caret.
Kunstler, G., Falster, D., Coomes, D.A., Hui, F., Kooyman, R.M., Laughlin, D.C., Poorter, L., Vanderwel, M., Vieilledent, G., Wright, S.J., Aiba, M., Baraloto, C., Caspersen, J., Cornelissen, J.H.C., Gourlet-Fleury, S., Hanewinkel, M., Herault, B., Kattge, J., Kurokawa, H., Onoda, Y., Peñuelas, J., Poorter, H., Uriarte, M., Richardson, S., Ruiz-Benito, P., Sun, I.-F., Ståhl, G., Swenson, N.G., Thompson, J., Westerlund, B., Wirth, C., Zavala, M.A., Zeng, H., Zimmerman, J.K., Zimmermann, N.E., Westoby, M., 2016. Plant functional traits have globally consistent effects on competition. Nature 529 (7585), 204–207.
Kuusk, A., 1991. In: Photon-Vegetation Interactions. Springer Berlin Heidelberg, Berlin, Heidelberg, pp. 139–159. https://doi.org/10.1007/978-3-642-75389-3_5.
Labate, D., Ceccherini, M., Cisbani, A., De Cosmo, V., Galeazzi, C., Giunti, L., Melozzi, M., Pieraccini, S., Stagi, M., 2009. The PRISMA payload optomechanical design, a high performance instrument for a new hyperspectral mission. Acta Astronaut. 65 (9-10), 1429–1436.
Landmann, T., Feilhauer, H., Shen, M., Chen, J., Raina, S., 2019. Mapping the Distribution and Abundance of Flowering Plants Using Hyperspectral Sensing. In: Advanced Applications in Remote Sensing of Agricultural Crops and Natural Vegetation. CRC Press, pp. 69–78. https://doi.org/10.1201/9780429431166-4.
Li, C., Wulf, H., Schmid, B., He, J.-S., Schaepman, M.E., 2018. Estimating plant traits of alpine grasslands on the qinghai-tibetan plateau using remote sensing. IEEE J. Sel. Top. Appl. Earth Observ. Remote Sens. 11 (7), 2263–2275.
Locherer, M., Hank, T.B., Danner, M., Mauser, W., 2015. Retrieval of seasonal leaf area index from simulated EnMAP data through optimized LUT-based inversion of the PROSAIL model. Remote Sens 7, 10321–10346.
Mevik, B.-H., Wehrens, R., Liland, K.H., 2018. pls: Partial Least Squares and Principal Component Regression. R Packag. version, 2.7-0.
Miraglio, T., Adeline, K., Huesca, M., Ustin, S.L., Briottet, X., 2020. Monitoring LAI, chlorophylls, and carotenoids content of a woodland savanna using hyperspectral imagery and 3D radiative transfer modeling. Remote Sens 12, 28.
Moreno-Martínez, Á., Camps-Valls, G., Kattge, J., Robinson, N., Reichstein, M., van Bodegom, P., Kramer, K., Cornelissen, J.H.C., Reich, P., Bahn, M., Niinemets, Ü., Peñuelas, J., Craine, J.M., Cerabolini, B.E.L., Minden, V., Laughlin, D.C., Sack, L., Allred, B., Baraloto, C., Byun, C., Soudzilovskaia, N.A., Running, S.W., 2018. A methodology to derive global maps of leaf traits using remote sensing and climate data. Remote Sens. Environ. 218, 69–88.
Pereira, H.M., Ferrier, S., Walters, M., Geller, G.N., Jongman, R.H.G., Scholes, R.J., Bruford, M.W., Brummitt, N., Butchart, S.H.M., Cardoso, A.C., Coops, N.C., Dulloo, E., Faith, D.P., Freyhof, J., Gregory, R.D., Heip, C., Hoft, R., Hurtt, G., Jetz, W., Karp, D.S., McGeoch, M.A., Obura, D., Onoda, Y., Pettorelli, N., Reyers, B., Sayre, R., Scharlemann, J.P.W., Stuart, S.N., Turak, E., Walpole, M., Wegmann, M., 2013. Essential biodiversity variables. Science 339 (6117), 277–278.
Pérez-Harguindeguy, N., Díaz, S., Garnier, E., Lavorel, S., Poorter, H., Jaureguiberry, P., Bret-Harte, M.S., Cornwell, W.K., Craine, J.M., Gurvich, D.E., Urcelay, C., Veneklaas, E.J., Reich, P.B., Poorter, L., Wright, I.J., Ray, P., Enrico, L., Pausas, J.G., de Vos, A.C., Buchmann, N., Funes, G., Quétier, F., Hodgson, J.G., Thompson, K., Morgan, H.D., ter Steege, H., van der Heijden, M.G.A., Sack, L., Blonder, B., Poschlod, P., Vaieretti, M.V., Conti, G., Staver, A.C., Aquino, S., Cornelissen, J.H.C., 2013. New handbook for standardised measurement of plant functional traits worldwide. Aust. J. Bot. 61, 167–234. https://doi.org/10.1071/BT12225.
R Core Team, 2018. R: A Language and Environment for Statistical Computing. R Found. Stat. Comput, Vienna, Austria https://www.R-project.org.
Roberts, D.A., Quattrochi, D.A., Hulley, G.C., Hook, S.J., Green, R.O., 2012. Synergies between VSWIR and TIR data for the urban environment: An evaluation of the potential for the Hyperspectral Infrared Imager (HyspIRI) Decadal Survey mission. Remote Sens. Environ. 117, 83–101.
Roelofsen, H.D., van Bodegom, P.M., Kooistra, L., Witte, J.P.M., 2013. Trait Estimation in Herbaceous Plant Assemblages from in situ Canopy Spectra. Remote Sens 5, 6323–6345.
Roosjen, P.P.J., Brede, B., Suomalainen, J.M., Bartholomeus, H.M., Kooistra, L., Clevers, J.G.P.W., 2018. Improved estimation of leaf area index and leaf chlorophyll content of a potato crop using multi-angle spectral data – Potential of unmanned aerial vehicle imagery. Int. J. Appl. Earth Obs. Geoinf. 66, 14–26.
Ryu, Y., Sonnentag, O., Nilson, T., Vargas, R., Kobayashi, H., Wenk, R., Baldocchi, D.D., 2010. How to quantify tree leaf area index in an open savanna ecosystem: A multi-instrument and multi-model approach. Agric. For. Meteorol. 150 (1), 63–76.
Savitzky, A., Golay, M.J.E., 1964. Smoothing and differentiation of data by simplified least squares procedures. Anal. Chem. 36 (8), 1627–1639.
Sehgal, V.K., Chakraborty, D., Sahoo, R.N., 2016. Inversion of radiative transfer model for retrieval of wheat biophysical parameters from broadband reflectance measurements. Inform. Process. Agric. 3 (2), 107–118.
Serbin, S.P., Wu, J., Ely, K.S., Kruger, E.L., Townsend, P.A., Meng, R., Wolfe, B.T., Chlus, A., Wang, Z., Rogers, A., 2019. From the Arctic to the tropics: multibiome prediction of leaf mass per area using leaf reflectance. New Phytol. 224 (4), 1557–1568.
Skidmore, A.K., Pettorelli, N., Coops, N.C., Geller, G.N., Hansen, M., Lucas, R., Mücher, C.A., O'Connor, B., Paganini, M., Pereira, H.M., Schaepman, M.E., Turner, W., Wang, T., Wegmann, M., 2015. Environmental science: Agree on biodiversity metrics to track from space. Nature 523 (7561), 403–405.
Stuffler, T., Kaufmann, C., Hofer, S., Förster, K.P., Schreier, G., Mueller, A., Eckardt, A., Bach, H., Penné, B., Benz, U., Haydn, R., 2007. The EnMAP hyperspectral imager – An advanced optical payload for future applications in Earth observation programmes. Acta Astronaut. 61 (1-6), 115–120.
Ustin, S.L., Gamon, J.A., 2010. Remote sensing of plant functional types. New Phytol. 186, 795–816. https://doi.org/10.1111/j.1469-8137.2010.03284.x.
Van Cleemput, E., Vanierschot, L., Fernández-Castilla, B., Honnay, O., Somers, B., 2018. The functional characterization of grass- and shrubland ecosystems using hyperspectral remote sensing: trends, accuracy and moderating variables. Remote Sens. Environ. 209, 747–763.
Verhoef, W., 1984. Light scattering by leaf layers with application to canopy reflectance modeling: The SAIL model. Remote Sens. Environ. 16 (2), 125–141.
Verhoef, W., Jia, L.i., Xiao, Q., Su, Z., 2007. Unified optical-thermal four-stream radiative transfer theory for homogeneous vegetation canopies. IEEE Trans. Geosci. Remote Sensing 45 (6), 1808–1822.
Verrelst, J., Camps-Valls, G., Muñoz-Marí, J., Rivera, J.P., Veroustraete, F., Clevers, J.G. P.W., Moreno, J., 2015. Optical remote sensing and the retrieval of terrestrial vegetation bio-geophysical properties – A review. ISPRS J. Photogramm. Remote Sens. 108, 273–290.
Verrelst, J., Malenovský, Z., Van der Tol, C., Camps-Valls, G., Gastellu-Etchegorry, J.-P., Lewis, P., North, P., Moreno, J., 2019. Quantifying vegetation biophysical variables from imaging spectroscopy data: A review on retrieval methods. Surv. Geophys. 40 (3), 589–629.

Vohland, M., Jarmer, T., 2008. Estimating structural and biochemical parameters for grassland from spectroradiometer data by radiative transfer modelling (PROSPECT+SAIL). Int. J. Remote Sens. 29 (1), 191–209.
Vohland, M., Mader, S., Dorigo, W., 2010. Applying different inversion techniques to retrieve stand variables of summer barley with PROSPECT+SAIL. Int. J. Appl. Earth Obs. Geoinf. 12 (2), 71–80.
von Humboldt, A., 1808. Ansichten der Natur. Tübingen.
Wang, Z., Townsend, P.A., Schweiger, A.K., Couture, J.J., Singh, A., Hobbie, S.E., Cavender-Bares, J., 2019. Mapping foliar functional traits and their uncertainties across three years in a grassland experiment. Remote Sens. Environ. 221, 405–416.
Wold, S., Sjöström, M., Eriksson, L., 2001. PLS-regression: A basic tool of chemometrics. Chemometr. Intell. Lab. Syst. 58 (2), 109–130.
Zarco-Tejada, P.J., Camino, C., Beck, P.S.A., Calderon, R., Hornero, A., Hernández-Clemente, R., Kattenborn, T., Montes-Borrego, M., Susca, L., Morelli, M., Gonzalez-Dugo, V., North, P.R.J., Landa, B.B., Boscia, D., Saponari, M., Navas-Cortes, J.A., 2018. Previsual symptoms of Xylella fastidiosa infection revealed in spectral plant-trait alterations. Nat. Plants 4 (7), 432–439.
Zhu, X., Skidmore, A.K., Darvishzadeh, R., Wang, T., 2019. Estimation of forest leaf water content through inversion of a radiative transfer model from LiDAR and hyperspectral data. Int. J. Appl. Earth Obs. Geoinf. 74, 120–129.